Macromolecules

ARTICLE

pubs.acs.org/Macromolecules

Ionic Conductivity of Nanostructured Block Copolymer/Ionic Liquid Membranes

Megan L. Hoarfrost[†,‡] and Rachel A. Segalman[*,†,§]

[†]Department of Chemical and Biomolecular Engineering, University of California, Berkeley, Berkeley, California 94720, United States

[‡]Energy and Environmental Technologies and [§]Materials Sciences Divisions, Lawrence Berkeley National Laboratory, Berkeley, California 94720, United States

Supporting Information

ABSTRACT: Nanostructured mixtures of ionic liquids and polymers are of great interest for a wide variety of electrochemical applications. Understanding the relationship between composition, structure, and ionic conductivity for these mixtures is essential for designing new materials. In this work, the effect of nanostructure on ionic conductivity, σ, is investigated for model mixtures of diblock copolymers and ionic liquids that are selective for one of the polymer microphases. It is demonstrated that the concentration dependence of σ is a function of the total volume fraction of ionic liquid and described well by percolation theory. This scaling behavior encourages the design of membranes where the amount of a mechanical component in the block copolymer can be increased to improve the strength of the membrane without sacrificing conductivity. The temperature dependence of σ is a function of the amount of ionic liquid exclusively in the conducting domain. Comparing σ for mixtures of the diblock copolymer poly(styrene-*block*-2-vinylpyridine) (S2VP) and two different ionic liquids, imidazolium bis(trifluoromethylsulfonyl)imide ([Im][TFSI]) and 1-ethyl-3-methylimidazolium bis(trifluoromethylsulfonyl)imide ([EMIm][TFSI]), reveals that the chemistry of the polymer/ionic liquid pair affects both the activation energy for σ and the maximum attainable σ but does not affect how σ scales with ionic liquid concentration. The effect of the morphology on σ is also examined, and it is found that as long as the conducting phase morphology is isotropic and well-connected, σ is not affected by morphology.

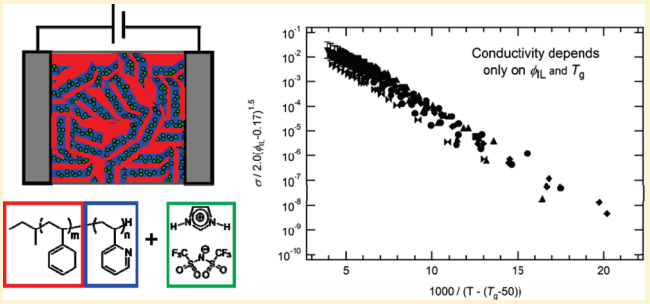

INTRODUCTION

Ionic liquids, which are salts with low melting temperatures or, equivalently, solvents composed completely of ions, have unique properties including low vapor pressure, high thermal, chemical, and electrochemical stability, and high ionic conductivity.[1] This exceptional combination of properties makes them of significant interest for a variety of electrochemical applications.[2] Combining ionic liquids with polymers is of further interest as the polymer may be designed to impart mechanical strength to the resulting membrane and template the ionic liquid into ion-conducting nanochannels. This can be achieved, for example, by selectively incorporating an ionic liquid into one phase of a diblock copolymer.[3,4]

When properly designed, nanostructured membranes feature continuous ion-conducting channels, which can lead to enhanced conductivity. Nafion (DuPont), the industry standard material for proton exchange membrane (PEM) fuel cell membranes, is characterized by nanoscale phase separation into conducting hydrophilic domains and structural hydrophobic domains, which contributes to exceptional conductivity coupled with favorable mechanical properties.[5] Model materials with continuous ordered nanostructures have also been shown to have significantly higher conductivities than comparable nonordered materials.[6,7] Understanding the effect of morphology on conductivity has become increasingly important in recent years as a tool for designing new, improved membranes.[8−12] Using a block copolymer to template the morphology provides an advantage because it affords precise control over the volume fractions of the conducting and structural phases and the size and shape of the domains.

In dilute electrolyte solutions, ionic conductivity, σ, is simply proportional to the number of ions and the diffusion coefficients of the ionic moieties (Nernst−Einstein equation). In concentrated mixtures of ionic liquids and compatible, neutral homopolymers, it is expected that σ does not scale linearly with the number of ions due to the effect of tortuosity and the need to be above a concentration threshold to form a percolated ionic liquid network. Also, the diffusion coefficients are greatly dependent on how far the temperature is above the glass transition temperature of the mixture, T_g,[13−15] where the T_g is actually a function of the

Received: January 11, 2011
Revised: April 21, 2011
Published: June 10, 2011

Table 1. Polymer Compositions and Morphologies of Block Copolymer/Ionic Liquid Mixtures

Polymers with Similar N_{P2VP}								
polymer	f_{PS}	N_{P2VP}	total MW (kg/mol)	PDI	$\varphi_{[Im][TFSI]}$	morphology	$\varphi_{[EMIm][TFSI]}$	morphology
P2VP	0.00	118	12.4	1.07	0.00 ≤ 0.61		0.00 ≤ 0.33	
S2VP	0.29	102	15.2	1.07	0.00 ≤ 0.52	C_{PS}	0.44	C_{PS}
					0.58 ≤ 0.71	$S_{PS,BCC}$		
S2VP	0.42	115	20.8	1.02	0.00 ≤ 0.17	LAM	0.00 ≤ 0.08	LAM
					0.21 ≤ 0.39	C_{PS}		
					0.48 ≤ 0.67	$S_{PS,FCC}$	0.14 ≤ 0.39	C_{PS}
					0.84	DM		
S2VP	0.62	108	29.8	1.10	0.00 ≤ 0.29	LAM		
					0.37	C_{PS}		
					0.58 ≤ 0.78	DM		
S2VP	0.72	101	39.2	1.04	0.05 ≤ 0.21	LAM		
					0.30 ≤ 0.72	DM		
Polymers with Similar f_{PS}								
polymer	f_{PS}	N_{P2VP}	total MW (kg/mol)	PDI	$\varphi_{[Im][TFSI]}$	morphology	$\varphi_{[EMIm][TFSI]}$	morphology
S2VP	0.62	108	29.8	1.10	0.00 ≤ 0.29	LAM		
					0.37	C_{PS}		
					0.58 ≤ 0.78	DM		
S2VP	0.62	221	61.7	1.10	0.26	LAM		
S2VP	0.59	296	75.8	1.10	0.27	LAM		
S2VP	0.65	451	135.0	1.19	0.24	LAM		

ionic liquid concentration.[16−18] Because the T_g typically decreases with increasing ionic liquid concentration,[16−18] and the number of ions simultaneously increases, the result is a monotonic increase in σ with increasing ionic liquid concentration.[18,19] This is also the case in nanostructured block copolymer membranes,[20,21] although ion concentration and T_g are not so intimately coupled. This is because the T_g is determined by the ionic liquid content exclusively in the conducting phase,[22] while the ion concentration depends on the total amount of ionic liquid in the membrane. In this work, the scaling of σ with temperature and composition is decoupled by varying the volume fraction of the structural component in the block copolymer as well as the ionic liquid content. Understanding in detail how conductivity depends on concentration and temperature will provide knowledge about important design parameters for highly conductive polymer/ionic liquid membranes.

Conductivity scaling behavior has been investigated for other types of nanostructured, ion-conducting, polymeric materials, but they are fundamentally different from the block copolymer/ionic liquid membranes. At first, lithium bis(trifluoromethylsulfonyl)imide (LiTFSI) salts in poly(ethylene oxide) (PEO)-based polymer electrolytes appear similar to ionic liquids that contain TFSI as the anion. However, in these systems, Li^+ ions are conducted by movement between oxygen atoms, making the polymer intimately involved in the conductivity mechanism.[23] Furthermore, the addition of LiTFSI salts tends to increase the polymer's T_g, leading to a maximum in conductivity with respect to salt concentration due to the competition between the increase in ion concentration and the concomitant increase in T_g upon the addition of salt.[24] Both hydrated and ionic liquid-containing[25−27] versions of sulfonated polyelectrolytes, like Nafion, are fundamentally different from polymer/ionic liquid membranes due to the presence of sulfonic acid sites, which donate conductive protons. In such materials, protons are conducted via protonation/deprotonation reactions. At high hydration levels, the conductivity of sulfonated polyelectrolytes scales with the percent conducting volume, while at lower hydration levels, the conductivity is a more complicated function of sulfonation level, humidity, and morphology.[9]

In this work, using a model block copolymer/ionic liquid system, we demonstrate that while the temperature dependence of σ is a function of the amount of ionic liquid exclusively in the conducting domain, the concentration dependence of σ is a function of the total volume fraction of ionic liquid. By comparing σ for mixtures of the diblock copolymer poly(styrene-*block*-2-vinylpyridine) (S2VP) and two different ionic liquids, imidazolium bis(trifluoromethylsulfonyl)imide ([Im][TFSI]) and 1-ethyl-3-methylimidazolium bis(trifluoromethylsulfonyl)imide ([EMIm][TFSI]), the universality of this scaling behavior is demonstrated. The effect of morphology on σ is also discussed, and it is shown that morphology does not strongly influence σ, as long as the conducting phase morphology is isotropic and well-connected.

EXPERIMENTAL SECTION

Polymer Synthesis and Characterization. S2VP copolymers and poly(2-vinylpyridine) (P2VP) homopolymer were synthesized via anionic polymerization as previously described.[28] The molecular weight of the polystyrene (PS) block was determined using gel permeation chromatography (GPC), and the total molecular weight of the block copolymer was determined via ^{1}H NMR (Bruker AVB-300 and Bruker DRX-500). The molecular weight of the P2VP homopolymer was determined using ^{1}H NMR end-group analysis. GPC was used to assess the polydispersity of the polymers. The volume fraction of the PS block, f_{PS}, degree of polymerization of the P2VP block, N_{P2VP}, total molecular weight,

MW, and polydispersity index, PDI, of the polymers are provided in Table 1. The structure of the S2VP copolymer is shown in Figure 1.

Ionic Liquid Purification and Preparation. Imidazole (≥95%) and bis(trifluoromethylsulfonyl)imide (HTFSI, ≥95%) were purchased from Sigma-Aldrich and purified by sublimation. Differential scanning calorimetry (DSC) and ^{1}H NMR were used to assess the purity of the two starting materials. The melting points of imidazole and HTFSI were compared to literature values of 89 and 55 °C, respectively.[29] To prepare the ionic liquid [Im][TFSI], purified imidazole and HTFSI were combined in equimolar quantities in an argon atmosphere glovebox, sealed, heated in an oven outside the glovebox at 100 °C for 2−3 h, and then transferred back to the glovebox. The composition of the ionic liquid was confirmed by comparing the measured melting point of the compound with the literature value of 73 °C.[29] The ionic liquid [EMIm][TFSI] was purchased from EMD Chemicals, Inc. and purified by heating at 100 °C under vacuum ($P \approx 200$ mTorr) for 3 days before it was transferred to an argon atmosphere glovebox. Care was taken to limit air and water exposure of the hydroscopic ionic liquids at all times by handling the materials in an argon atmosphere glovebox and sealed sample holders. The structures of the ionic liquid ions are shown in Figure 1.

Preparation of Polymer/Ionic Liquid Mixtures. Dichloromethane and tetrahydrofuran were degassed using three freeze−pump−thaw cycles, dried by stirring over CaH_2 overnight, then distilled under vacuum, brought into an argon atmosphere glovebox, and stored on molecular sieves. All further sample preparation was performed in an argon atmosphere glovebox. Specific quantities of [Im][TFSI] or [EMIm][TFSI] and S2VP or P2VP were weighed into glass vials and were dissolved overnight in dichloromethane (S2VP mixtures) or tetrahydrofuran (P2VP mixtures) to produce ca. 5 wt % solutions. Samples were cast one drop at a time into sample holders for DSC, small-angle X-ray scattering (SAXS), and ac impedance spectroscopy. Samples were then heated above the boiling point of the solvent (65 and 70 °C for samples cast from dichloromethane and tetrahydrofuran, respectively) for ca. 18 h to remove any remaining solvent. Complete solvent removal was confirmed by ^{1}H NMR analysis and the achievement of constant sample mass. Samples were sealed in jars containing desiccant in the glovebox for transportation to experimental apparatuses.

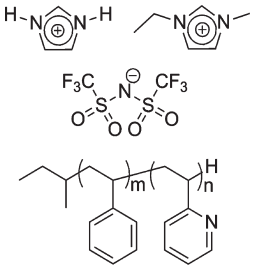

Figure 1. Chemical structures of imidazolium, 1-ethyl-3-methylimidazolium, and TFSI ions (top left, top right, and middle, respectively) and S2VP copolymer (bottom).

Differential Scanning Calorimetry (DSC). DSC samples were crimped in an argon atmosphere glovebox using hermetically sealed pans and placed inside a container with desiccant for transfer to the DSC. DSC was performed on a TA Instruments DSC Q20. Indium and dodecane were used as calibration standards. Samples underwent three heating and cooling cycles between −40 and 150 °C, scanning at 10 °C/min, and T_g values recorded upon the second heating scan are reported.

Morphology Characterization. Mixture morphologies were determined using SAXS. Samples were cast in an argon atmosphere glovebox into sample cells formed by an aluminum spacer sealed onto a Kapton window on one side until ca. 1 mm solid samples were obtained. After heating to remove solvent, a second Kapton window was glued to seal the samples, and the samples were stored in jars containing desiccant for transportation to the beamline. SAXS was performed on beamline 7.3.3 of the Advanced Light Source (ALS) and beamline 1-4 of the Stanford Synchrotron Radiation Lightsource (SSRL). At the ALS, the beamline was configured with an X-ray wavelength of λ = 1.240 Å and focused to a 50 by 300 μm spot. Samples were annealed and equilibrated at 145 °C for 20−30 min prior to data acquisition. Full two-dimensional scattering patterns were collected on an ADSC CCD detector with an active area of 188 by 188 mm. The scattering patterns, which reflected isotropic structures in all cases, were radially averaged, and the scattering intensity was corrected with the postion chamber intensity using Nika version 1.18. At the SSRL, the beamline was configured with an X-ray wavelength λ = 1.488 Å and focused to a 0.5 mm diameter spot. A single quadrant of a two-dimensional scattering pattern was collected on a CCD detector with an active area of 25.4 by 25.4 mm. The scattering patterns, which reflected isotropic structures in all cases, were radially averaged and corrected for detector null signal, dark current, and empty cell scattering.

The S2VP/[Im][TFSI] samples in this study exhibit a variety of morphologies, including lamellae (LAM), hexagonally close-packed (HCP) PS cylinders (C_{PS}), body-centered cubic (BCC) PS spheres ($S_{PS,BCC}$), face-centered cubic (FCC) PS spheres ($S_{PS,FCC}$), and disordered PS micelles (DM), as determined by analysis of SAXS profiles reported in ref 22. For each copolymer, the morphologies are

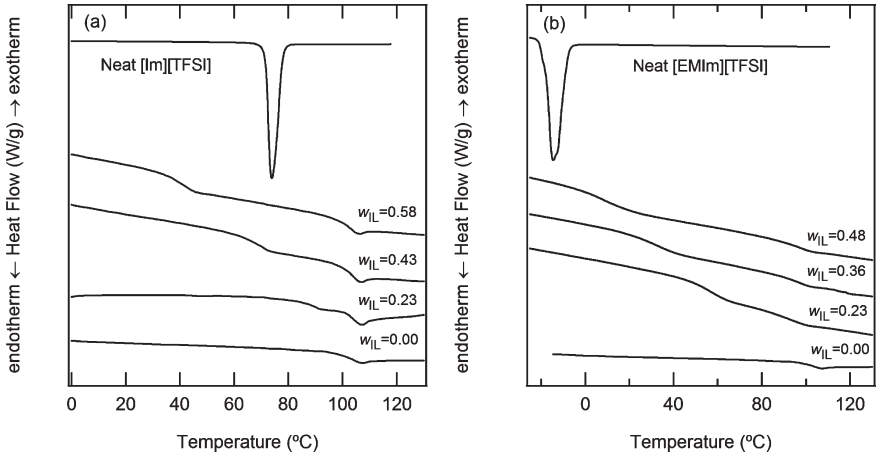

Figure 2. Representative DSC heating scans for (a) S2VP(f_{PS} = 0.72)/[Im][TFSI] mixtures and (b) S2VP(f_{PS} = 0.42)/[EMIm][TFSI] mixtures.

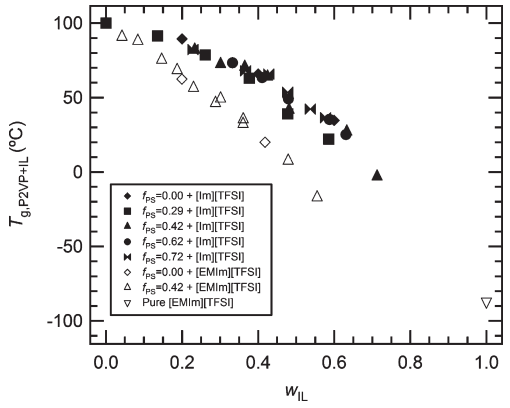

Figure 3. $T_{g,P2VP+IL}$ as a function of w_{IL} for S2VP copolymers and P2VP homopolymer mixed with [Im][TFSI] and [EMIm][TFSI]. All T_g values were determined using DSC except for the T_g of [EMIm][TFSI], which is from ref 31.

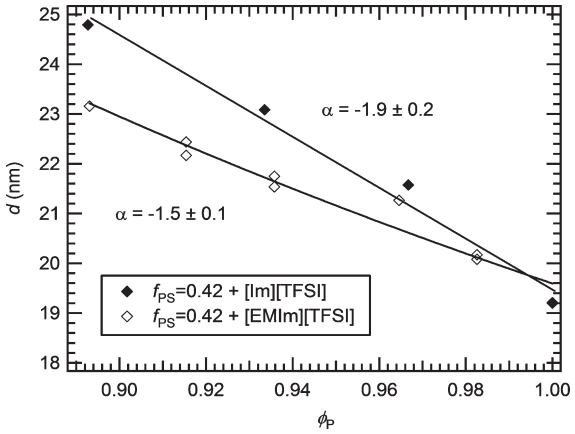

Figure 4. Lamellar domain spacing, d, determined from SAXS at 145 °C as a function of φ_P for S2VP(f_{PS} = 0.42)/[Im][TFSI] mixtures (solid symbols) and S2VP(f_{PS} = 0.42)/[EMIm][TFSI] mixtures (open symbols). Power law fits, $d \sim \varphi_P^{\alpha}$, are used to obtain α, and the errors represent one standard deviation of the fits.

provided in Table 1 as a function of the total volume fraction of [Im][TFSI] in the mixtures, $\varphi_{[Im][TFSI]}$. The S2VP/[EMIm][TFSI] samples in this study have LAM and C_{PS} morphologies, as determined from analysis of SAXS measurements. Representative SAXS profiles for mixtures of S2VP and [EMIm][TFSI] are plotted in Figures S1 and S2 of the Supporting Information, and the morphologies are provided as a function of $\varphi_{[EMIm][TFSI]}$ in Table 1.

Selectivity of Ionic Liquids for P2VP. It has been previously shown that [Im][TFSI] is very selective for the P2VP phase of S2VP copolymers,[22,30] and the same is true of [EMIm][TFSI]. This is reflected in the thermal properties of the mixtures. As shown in Figure 2, upon the addition of [Im][TFSI] and [EMIm][TFSI] to S2VP copolymers, the T_g of the ionic liquid-containing P2VP phase, $T_{g,P2VP+IL}$, decreases from that of neat P2VP. $T_{g,P2VP+IL}$ collapses for all copolymers as a function of the weight fraction of ionic liquid exclusively in the P2VP phase, w_{IL}, as shown in Figure 3. The T_g of the PS domain, however, remains in the vicinity of 100 °C with increasing w_{IL} as expected because the ionic liquid selectively enters the P2VP domain. The degree of selectivity of the ionic liquids for the P2VP phase is quantified and found to be very high based on the scaling behavior of the domain spacing of self-assembled microdomains, d, with volume fraction polymer, φ_P. In Figure 4, d is plotted as a function of φ_P for lamellar S2VP(f_{PS} = 0.72)/[Im][TFSI] and S2VP(f_{PS} = 0.42)/[EMIm][TFSI] mixtures. d was calculated as $2\pi/q^*$, where q^* is the primary scattering peak from SAXS data. Power law fits through each set of data, $d \sim \varphi_P^{\alpha}$, result in α = −1.9 and −1.5 for S2VP(f_{PS} = 0.72)/[Im][TFSI] and S2VP(f_{PS} = 0.42)/[EMIm][TFSI], respectively. Values of α < 0 (d increases upon the addition of ionic liquid) indicate that [Im][TFSI] and [EMIm][TFSI] are both selective for one block of the copolymer.[32] Values of −1.9 and −1.5 for α are both very negative compared to values observed for typical block copolymer/selective molecular solvent mixtures,[22] indicating that [Im][TFSI] and [EMIm][TFSI] are both strongly selective for P2VP. Because of the strong selectivity of the systems, S2VP/[Im][TFSI] and S2VP/[EMIm][TFSI] are good model systems for studying block copolymer/ionic liquid mixtures. In addition, the strong selectivities substantiate the simplifying assumption that all ionic liquid enters the P2VP phase of S2VP copolymers. Samples are designated by w_{IL} as well as the total volume fraction of ionic liquid, φ_{IL}, which is calculated by assuming ideal mixing and using densities of 1.67 g/cm^3 for [Im][TFSI], estimated from scattering length density fits of small-angle neutron scattering intensity profiles,[30] 1.52 g/cm^3 for [EMIm][TFSI],[33] and 1.05 g/cm^3 for both PS and P2VP.

Ionic Conductivity Measurements. Ionic conductivity was measured using ac impedance spectroscopy. In an argon atmosphere glovebox, samples were cast onto stainless steel blocking electrodes. After heating to remove remaining solvent, two sample-coated electrodes were sandwiched together with an annular Kapton spacer placed in between with a thickness of 25 μm and an inner diameter of 1.4 cm. The sandwiches were pressed at 105 °C for 1 h in the glovebox using a hand press to allow the samples to completely fill the Kapton spacers. The samples were then placed in homemade, airtight, stainless steel cells with Teflon flanges. The cells were screwed together in the glovebox, clamped to maintain constant pressure, and then annealed at 150 °C for 12 h in an oven outside the glovebox prior to performing measurements. Two-point probe, through-plane ac impedance measurements were performed using a Gamry Reference 600 potentiostat at descending temperatures. An alternating current signal with an amplitude of 5 mV was applied in the frequency range of 100−65000 Hz. Nyquist plots of the negative imaginary part of the impedance, $-Z''$, versus the real part of the impedance, Z', were analyzed to find the sample resistance, R. Typically, Z' at the minimum in the Nyquist plot (the high x-intercept of the semicircle portion of the data) was taken as R. For highly conductive samples, the semicircle portion of the data was not observed in the frequency range of the potentiostat, so the x-intercept was taken as R. Representative Nyquist plots for each scenario are shown in Figure S3 of the Supporting Information. The ionic conductivity, σ, was calculated as t/AR, where t and A are the thickness and area of the sample, respectively, measured after the ac impedance measurements. Specifically, t was determined by measuring the total thickness of the membrane/spacer/electrodes sandwich and subtracting the thicknesses of the electrodes.

Four-point probe measurements in the in-plane direction were performed to confirm that σ was isotropic. For the four-point probe measurements, samples were cast and hot-pressed in the same manner as the samples measured using two-point probe ac impedance, but into a homemade, airtight, poly(ether ether ketone) cell, which contained four stainless steel electrodes and was screwed shut in an argon atmosphere glovebox. The working and reference electrodes were 0.7 cm apart and 1.9 cm long, and the samples were cast to be about 0.05 cm thick. The ac impedance spectroscopy parameters were the same as the parameters used for the two-point probe, through-plane measurements, and σ was calculated in the same manner. Values of σ measured using four-point probe measurements were comparable to those measured using two-point probe measurements, confirming isotropic conductivity. Two-point probe measurements are reported.

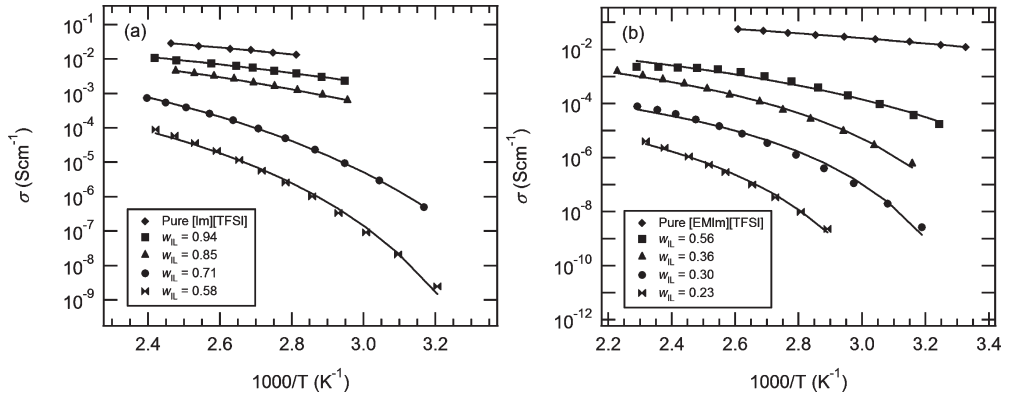

Figure 5. Temperature dependence of σ for (a) S2VP(f_{PS} = 0.62, N_{P2VP} = 108)/[Im][TFSI] mixtures and (b) S2VP(f_{PS} = 0.42)/[EMIm][TFSI] mixtures with many w_{IL}. The solid lines are VTF fits with A and B as fitting parameters and $T_0 = T_{g,P2VP+IL} - 50$ K. The best fit values for B are 8.1 ± 1.2 kJ/mol for S2VP/[ImTFSI] and 6.8 ± 1.2 kJ/mol for S2VP/[EMIm][TFSI].

RESULTS AND DISCUSSION

Ionic Conductivity of S2VP/[Im][TFSI]. For mixtures of S2VP block copolymers and [Im][TFSI], σ increases with increasing w_{IL}, and the temperature dependence of σ becomes less steep with increasing w_{IL}, as shown for representative mixtures in Figure 5. There are two factors contributing to this behavior: the increase in ion concentration with increasing w_{IL} and the decrease in $T_{g,P2VP+IL}$ with increasing w_{IL}. ($T_{g,P2VP+IL}$ is the important T_g that affects ion mobility since all of the ions reside in and travel through the ionic liquid-containing P2VP phase.) Quantitatively, this translates into an expression for σ with a concentration dependence in terms of the overall volume fraction of ionic liquid, φ_{IL}, and a temperature dependence that is in terms of T and w_{IL}. Separation of the temperature and concentration dependencies of σ was accomplished by evaluating σ versus temperature data for mixtures of [Im][TFSI] and S2VP copolymers (listed in Table 1) with similar N_{P2VP} but various f_{PS}. In this manner, φ_{IL} and w_{IL} were tuned independently by varying the block copolymer composition (f_{PS}) and ionic liquid content.

The strong influence of the T_g on ionic conductivity is reflected in the Vogel−Tamman−Fulcher (VTF) equation[34−37]

$$\sigma = A \exp\left(\frac{-B}{R(T - T_0)}\right) \qquad (1)$$

where A is a fitting parameter that contains the concentration dependence of σ, B contains information about the temperature dependence of σ, and T_0 is the Vogel temperature. While T_0 for polymers has been shown to fluctuate with respect to T_g, a good estimate for T_0 is about 50 K below T_g.[38−40] Assuming $T_0 = T_{g,P2VP+IL} - 50$ K is a good choice, it is expected that one value for B will be obtained for all of the S2VP/[Im][TFSI] mixtures. As expected, for 24 mixtures of [Im][TFSI] and S2VP copolymers with different f_{PS} and w_{IL}, the VTF fits (shown in Figure 5) result in similar best fits for B: 8.1 kJ/mol with a standard deviation of 1.2 kJ/mol. Therefore, $T_{g,P2VP+IL}$ (which is a function of w_{IL}) is the only factor that determines the temperature dependence of σ for S2VP/[Im][TFSI] mixtures.

While the temperature dependence of σ is determined by the amount of ionic liquid exclusively in the conducting domain, w_{IL}, the concentration dependence of σ is a function of the *total* volume fraction of ionic liquid in the system, φ_{IL}. This is shown in Figure 6, where the fitting parameter A from eq 1 collapses as a function of φ_{IL} for S2VP/[Im][TFSI] mixtures containing block copolymers with many different f_{PS} (and, thus, w_{IL}) and over a wide range of φ_{IL}. In other words, at sufficiently high temperatures, where the dependence of σ on ion concentration is much more important than it is on temperature, similar conductivities are obtained for mixtures containing block copolymers of widely different compositions as long as φ_{IL} is kept constant. Figure 7 shows that σ is a strong function of φ_{IL} even at temperatures as low as 100 °C. This is an important result to take into account when designing new materials based on mixtures of polymers and ionic liquids, since it means that polymers with high volume fractions of a structural component can be used to impart good mechanical properties without sacrificing ionic conductivity. For example, a lamellar mixture of S2VP(f_{PS} = 0.72) and [Im][TFSI] with φ_{IL} = 0.20 will have roughly the same ionic conductivity at high temperatures as a mixture of P2VP and [Im][TFSI] with φ_{IL} = 0.20, even though more than half of the total volume in the block copolymer sample is composed of the structural PS phase. Interestingly, this scaling behavior is similar to that of sulfonated polyelectrolytes at high hydration levels, where conductivity has

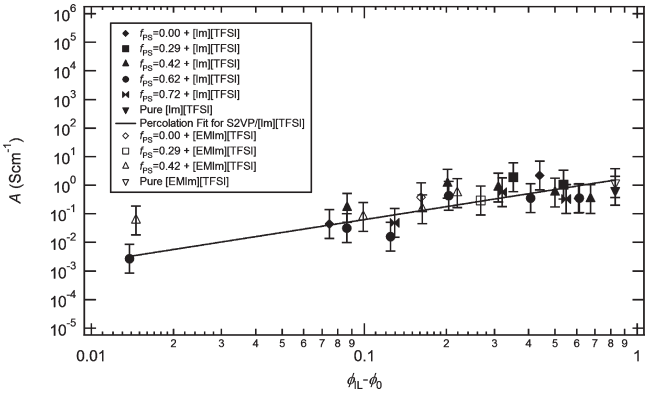

Figure 6. A, determined by VTF fits with A and B as fitting parameters and $T_0 = T_{g,P2VP+IL} - 50$ K, as a function of $\varphi_{IL} - \varphi_0$ for S2VP/[Im]-[TFSI] mixtures (solid symbols) and S2VP/[EMIm][TFSI] mixtures (open symbols). φ_0 is the percolation threshold for conductivity. The error bars represent reasonable estimates based on the accuracy of ac impedance measurements and data fits. The solid line is the percolation model fit to S2VP/[Im][TFSI] data with n = 1.5 and φ_0 and σ_0 as fitting parameters.

dx.doi.org/10.1021/ma200060g |*Macromolecules* 2011, 44, 5281–5288

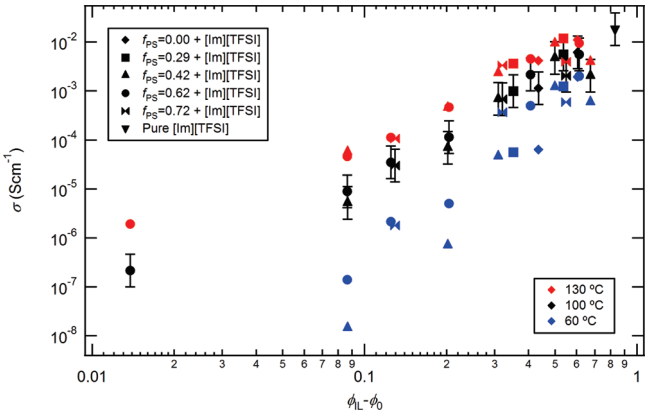

Figure 7. σ versus $\varphi_{IL} - \varphi_0$ for S2VP/[Im][TFSI] mixtures at 130 °C (red symbols), 100 °C (black symbols), and 60 °C (blue symbols). φ_0 is the percolation threshold for conductivity. Error bars represent reasonable estimates based on the accuracy of ac impedance measurements and are shown only for 100 °C data for clarity.

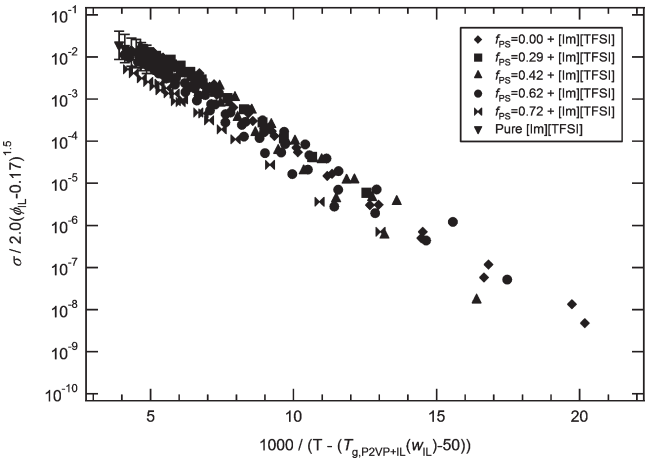

Figure 8. Conductivity data for all S2VP/[Im][TFSI] samples, plotted according to eq 3. For graphical clarity, the error bars are shown only for pure [Im][TFSI]. They represent a reasonable estimate based on the accuracy of ac impedance measurements and can be extended to all data points.

been shown to collapse as a function of percent conducting volume.[9] At lower temperatures, however, for instance 60 °C (Figure 7), conductivity is a weaker function of φ_{IL} due to the stronger effect of $T_{g,P2VP+IL}$.

The fitting parameter A clearly increases nonlinearly with increasing φ_{IL}, which is due to the effects of tortuosity and the need to be above a concentration threshold to form a percolated ionic liquid network. The concentration dependence of σ for S2VP/[Im][TFSI] is modeled well using percolation theory, specifically the power law

$$A = \sigma_0(\varphi_{IL} - \varphi_0)^n \quad (2)$$

where the prefactor σ_0 depends on the system, φ_0 is the percolation threshold volume fraction, and the exponent n is a constant that includes the effect of tortuosity, depends only on the spatial dimensions, and is 1.5 for a 3-D system.[41,42] For an ideal, continuous, 3-D system, φ_0 = 0.15,[43] but φ_0 is easily influenced by the distribution of the conductive phase, as occurs in the case of Nafion, where phase separation causes a percolated hydrophilic network to be formed at low water concentrations (φ_0 = 0.06).[44] For the S2VP/[Im][TFSI] system, the best fit values for σ_0 and φ_0 are 2.0 ± 1.1 S/cm and 0.17 ± 0.02, respectively. The percolation fit is shown in Figure 6. Within error, the best fit value for φ_0 matches that of the ideal 3-D system. Thus, self-assembly of S2VP/[Im][TFSI] mixtures in this study does not lead to a decrease in φ_0 compared to the ideal 3-D case as the phase separation of Nafion does. The percolation behavior of A versus φ_{IL} should be taken into account when designing new materials based on polymers and ionic liquids. Because mechanical properties are expected to worsen with increasing ionic liquid concentration, perhaps the nonlinear conductivity dependence on φ_{IL} can be exploited in determining an optimal membrane ionic liquid concentration.

Combining the temperature and concentration dependencies of σ for mixtures of S2VP and [Im][TFSI] results in an equation for the conductivity of any S2VP/[Im][TFSI] mixture:

$$\sigma = 2.0(\varphi_{IL} - 0.17)^{1.5} \exp\left\{\frac{-8.1}{R[T - (T_{g,P2VP+IL}(w_{IL}) - 50)]}\right\} \quad (3)$$

The conductivity data for all S2VP/[Im][TFSI] samples are plotted according to eq 3 in Figure 8. While certain parameters in eq 3, for instance σ_0 = 2.0 S/cm, B = 8.1 kJ/mol, and $T_g(w_{IL})$, are specific to the model S2VP/[Im][TFSI] system, it is expected that the general form of the equation is applicable to other polymer/ionic liquid systems as well.

Morphology does not significantly impact the conductivity of S2VP/[Im][TFSI] mixtures for a variety of reasons. Phase contrast is high as [Im][TFSI] is strongly selective for the P2VP phase, and the system is strongly segregated.[22] Second, there is no preferential alignment of any of the morphologies relative to the electrodes, as indicated by radially symmetric SAXS patterns and similar σ measurements in both in-plane and through-plane directions. Finally, the wide variety of morphologies demonstrated by the mixtures, including lamellae, HCP PS cylinders, BCC and FCC PS spheres, and DM, can all be characterized as having conducting phase continuity, assuming the P2VP/ionic liquid domains in the lamellar samples are well-connected. Scatter in the data for σ is unrelated to the morphology exhibited, as clearly demonstrated in Figure S4 of the Supporting Information. Conductivity, then, is unaffected by morphology as long as the conducting phase is well-connected throughout the membrane, and the nanostructure is strongly segregated and isotropic. It is likely that if any of these conditions were not met, σ would not be described by eq 3.[6−9,45,46]

The S2VP/[Im][TFSI] mixtures discussed thus far have only included mixtures with copolymers having N_{P2VP} = 113 ± 12. It is expected that conductivity will be independent of P2VP molecular weight as long as it is high enough that $T_{g,P2VP}$ is independent of molecular weight.[13−15] Indeed, for mixtures containing S2VP with similar f_{PS} (0.62 ± 0.03) and various N_{P2VP} (108 ≤ N_{P2VP} ≤ 451), molecular weight does not affect σ, as shown in Figure 9.

Universality of Ionic Conductivity of Block Copolymer/Ionic Liquid Mixtures. The universality of the conductivity behavior of block copolymer/ionic liquid mixtures has been investigated by comparing σ of S2VP/[Im][TFSI] to that of mixtures of S2VP and a second ionic liquid, [EMIm][TFSI]. Changing the cation in the ionic liquid from imidazolium to

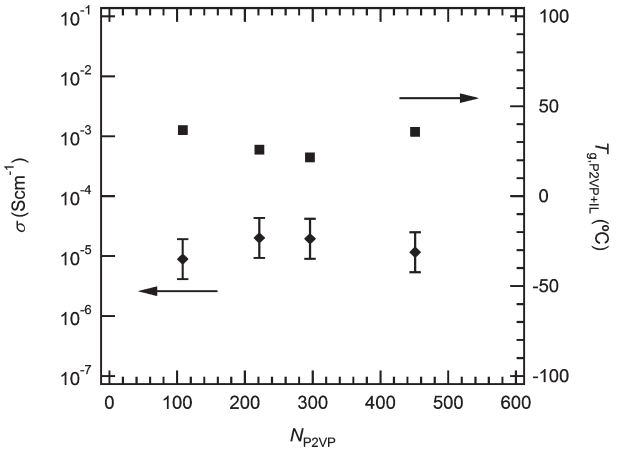

Figure 9. σ and $T_{g,P2VP+IL}$ as a function of N_{P2VP} for S2VP/[Im][TFSI] mixtures with f_{PS} = 0.62 ± 0.03, φ_{IL} = 0.25 ± 0.02, and T = 100 °C.

1-ethyl-3-methylimidazolium results in changes in the temperature dependence of σ and the maximum conductivity of the mixtures but does not change the overall scaling relationships between σ, φ_{IL}, w_{IL}, and T. Consequently, the chemistry of mixtures of block copolymers and ionic liquids can be tuned to improve ionic conductivity while still taking advantage of design parameters universal to all chemistries.

Equation 1, which was used to model σ of S2VP/[Im][TFSI] mixtures, also describes the S2VP/[EMIm][TFSI] data well (Figure 5). Furthermore, B collapses for all of the S2VP/[EMIm][TFSI] mixtures with $T_0 = T_{g,P2VP+IL} - 50$ K, just like in the S2VP/[Im][TFSI] system, confirming the generality of the conclusion that the temperature dependence of σ is only a function of the T_g of the conducting phase in block copolymer/ionic liquid mixtures (within mixtures of a given chemistry). The relationship between $T_{g,P2VP}$ and w_{IL}, though, is different for the two systems. As shown in Figure 3, while $T_{g,P2VP}$ collapses as a function of w_{IL} for each type of mixture, $T_{g,P2VP}$ decreases more rapidly with w_{IL} for S2VP/[EMIm][TFSI] mixtures compared to S2VP/[Im][TFSI] mixtures. Also, the chemistry of the system affects the value of B. The best fit value of B for S2VP/[EMIm][TFSI] is 6.8 kJ/mol with a standard deviation of 1.0 kJ/mol compared to 8.1 kJ/mol with a standard deviation of 1.2 kJ/mol for S2VP/[Im][TFSI]. One likely contributor to S2VP/[EMIm][TFSI] mixtures exhibiting a lower B value is the existence of different P2VP/ionic liquid interactions in each type of mixture. Unlike [EMIm][TFSI], [Im][TFSI] is protic and likely participates in hydrogen bonding with and protonation of 2VP monomers, slowing down the transport of imidazolium cations compared to ethylmethylimidazolium cations. Another possibility is that ion aggregation occurs to varying degrees as a function of temperature and w_{IL} in the S2VP/[Im][TFSI] and S2VP/[EMIm][TFSI] systems.[18,47] The extent of ion aggregation in the S2VP/ionic liquid membranes is the subject of future work. Thus, to maximize conductivity at a given temperature and φ_{IL}, a block copolymer and ionic liquid pair should be chosen such that the T_g of the host copolymer phase is low and/or greatly depressed upon addition of ionic liquid, and so that B is low.

Percolation theory, which describes the concentration dependence of σ for S2VP/[Im][TFSI] mixtures, also describes the S2VP/[EMIm][TFSI] data well (Figure 6), suggesting that the concentration dependence of σ being a function of φ_{IL} is a general property of mixtures of block copolymers and ionic liquids, at least in systems where morphology does not significantly influence conductivity. It is expected that φ_0 and n in eq 2 will be similar for both types of mixtures since they are properties of the geometry of the system, which is confirmed by the S2VP/[EMIm][TFSI] data points falling very close to the percolation curve fit for S2VP/[Im][TFSI] mixtures. The value of σ_0 depends on the system and should be different for each type of mixture. The fact that σ_0 does not appear to be significantly different for S2VP/[Im][TFSI] and S2VP/[EMIm][TFSI] most likely reflects the similar ionic conductivities of neat [Im][TFSI] and [EMIm][TFSI].[29,31]

In summary, the general form of eq 3

$$\sigma = \sigma_0(\varphi_{IL} - 0.17)^{1.5} \exp\left\{\frac{-B}{R[T - (T_g(w_{IL}) - 50)]}\right\} \quad (4)$$

is predicted to be widely applicable to block copolymer/ionic liquid systems, where the tunable parameters are $T_g(w_{IL})$ and B, which are characteristic of the polymer/ionic liquid pair, and σ_0, which is characteristic of the ionic liquid. It is emphasized that eq 4 is applicable only to systems where the conducting phase morphology is well-connected, isotropic, and strongly segregated from the structural phase.

CONCLUSION

Phase-separated mixtures of ionic liquids and polymers are of great interest for a wide variety of electrochemical applications. Understanding the relationship between polymer composition, ionic liquid concentration, temperature, and ionic conductivity for these mixtures is essential for designing new materials. In this work, the concentration and temperature dependencies of σ for model mixtures of S2VP block copolymers and [Im][TFSI] and [EMIm][TFSI] ionic liquids have been successfully decoupled. While the temperature dependence of σ is a function of $T_{g,P2VP+IL}$, which is a function of the amount of ionic liquid exclusively in the P2VP domain of the block copolymer, the concentration dependence of σ is a function of the overall volume fraction of ionic liquid, φ_{IL}. This scaling behavior allows for the design of membranes where the amount of a mechanical component in the block copolymer can be increased to improve the strength of the membrane without sacrificing conductivity (as long as φ_{IL} is kept high). The chemistry of the system can also be tuned to increase σ at a given temperature and φ_{IL} by selecting a block copolymer/ionic liquid pair for which the T_g of the ionic liquid host phase is low and/or greatly depressed upon the addition of ionic liquid and for which the neat ionic liquid has a high σ. Molecular weight and morphology, as long as the conducting phase is isotropic and well-connected, have been found to have negligible effects on σ.

ASSOCIATED CONTENT

Supporting Information. SAXS profiles of representative S2VP/[EMIm][TFSI] mixtures, representative Nyquist plots, and A versus $\varphi_{IL} - \varphi_0$ labeled by morphology. This material is available free of charge via the Internet at http://pubs.acs.org.

AUTHOR INFORMATION

Corresponding Author
*E-mail: segalman@berkeley.edu.

ACKNOWLEDGMENT

We gratefully acknowledge support from the Assistant Secretary for Energy Efficiency and Renewable Energy, Office of Hydrogen, Fuel Cell, and Infrastructure Technologies of the U.S. Department of Energy under Contract DE-AC02-05CH11231. The authors thank Prof. Nitash Balsara, Dr. John Kerr, Dr. Justin Virgili, Dr. Adam Weber, and Prof. John Newman for many useful discussions. SAXS experiments were performed at the Advanced Light Source (ALS) and the Stanford Synchrotron Radiation Lightsource (SSRL). Both are national user facilities supported by the Department of Energy, Office of Basic Energy Sciences. We gratefully acknowledge Dr. Alexander Hexemer, Dr. Cheng Wang, and Dr. Eric Schaible for experimental assistance at the ALS and Dr. John Pople for experimental assistance at the SSRL.

REFERENCES

(1) Wasserscheid, P.; Welton, T. *Ionic Liquids in Synthesis*; Wiley-VCH Verlag: Weinheim, 2003.
(2) Ohno, H. *Electrochemical Aspects of Ionic Liquids*; Wiley-Interscience: New York, 2005.
(3) Simone, P. M.; Lodge, T. P. *Macromolecules* **2008**, *41* (5), 1753–1759.
(4) Virgili, J. M.; Hexemer, A.; Pople, J. A.; Balsara, N. P.; Segalman, R. A. *Macromolecules* **2009**, *42* (13), 4604–4613.
(5) Mauritz, K. A.; Moore, R. B. *Chem. Rev.* **2004**, *104* (10), 4535–4585.
(6) Chen, Y. B.; Thorn, M.; Christensen, S.; Versek, C.; Poe, A.; Hayward, R. C.; Tuominen, M. T.; Thayumanavan, S. *Nature Chem.* **2010**, *2* (6), 503–508.
(7) Ichikawa, T.; Yoshio, M.; Hamasaki, A.; Mukai, T.; Ohno, H.; Kato, T. *J. Am. Chem. Soc.* **2007**, *129* (35), 10662.
(8) Cho, B. K.; Jain, A.; Gruner, S. M.; Wiesner, U. *Science* **2004**, *305* (5690), 1598–1601.
(9) Kim, Y. S.; Pivovar, B. S. *Annu. Rev. Chem. Biomol. Eng.* **2010**, *1*, 123–148.
(10) Rubatat, L.; Li, C. X.; Dietsch, H.; Nykanen, A.; Ruokolainen, J.; Mezzenga, R. *Macromolecules* **2008**, *41* (21), 8130–8137.
(11) Ruzette, A. V. G.; Soo, P. P.; Sadoway, D. R.; Mayes, A. M. *J. Electrochem. Soc.* **2001**, *148* (6), A537–A543.
(12) Wanakule, N. S.; Panday, A.; Mullin, S. A.; Gann, E.; Hexemer, A.; Balsara, N. P. *Macromolecules* **2009**, *42* (15), 5642–5651.
(13) Fujita, H.; Kishimoto, A.; Matsumoto, K. *Trans. Faraday Soc.* **1960**, *56* (3), 424–437.
(14) Vrentas, J. S.; Duda, J. L. *J. Polym. Sci., Part B: Polym. Phys.* **1977**, *15* (3), 403–416.
(15) Vrentas, J. S.; Duda, J. L. *J. Polym. Sci., Part B: Polym. Phys.* **1977**, *15* (3), 417–439.
(16) Lodge, T. P.; Mok, M. M.; Liu, X. C.; Bai, Z. F.; Lei, Y. *Macromolecules* **2011**, *44* (4), 1016–1025.
(17) Scott, M. P.; Brazel, C. S.; Benton, M. G.; Mays, J. W.; Holbrey, J. D.; Rogers, R. D. *Chem. Commun.* **2002**, No. 13, 1370–1371.
(18) Susan, M. A.; Kaneko, T.; Noda, A.; Watanabe, M. *J. Am. Chem. Soc.* **2005**, *127* (13), 4976–4983.
(19) Seki, S.; Susan, A. B. H.; Kaneko, T.; Tokuda, H.; Noda, A.; Watanabe, M. *J. Phys. Chem. B* **2005**, *109* (9), 3886–3892.
(20) Simone, P. M.; Lodge, T. P. *ACS Appl. Mater. Interfaces* **2009**, *1* (12), 2812–2820.
(21) Winey, K. I.; Gwee, L.; Choi, J. H.; Elabd, Y. A. *Polymer* **2010**, *51* (23), 5516–5524.
(22) Virgili, J. M.; Hoarfrost, M. L.; Segalman, R. A. *Macromolecules* **2010**, *43* (12), 5417–5423.
(23) Gray, F. M. *Solid Polymer Electrolytes: Fundamentals and Technological Applications*; VCH Publishers, Inc.: New York, 1991.
(24) Robitaille, C. D.; Fauteux, D. *J. Electrochem. Soc.* **1986**, *133* (2), 315–325.
(25) Cho, E.; Park, J. S.; Sekhon, S. S.; Park, G. G.; Yang, T. H.; Lee, W. Y.; Kim, C. S.; Park, S. B. *J. Electrochem. Soc.* **2009**, *156* (2), B197–B202.
(26) Doyle, M.; Choi, S. K.; Proulx, G. *J. Electrochem. Soc.* **2000**, *147* (1), 34–37.
(27) Kim, S. Y.; Kim, S.; Park, M. J. *Nature Commun.* **2010**, 1.
(28) Yokoyama, H.; Mates, T. E.; Kramer, E. J. *Macromolecules* **2000**, *33* (5), 1888–1898.
(29) Noda, A.; Susan, A. B.; Kudo, K.; Mitsushima, S.; Hayamizu, K.; Watanabe, M. *J. Phys. Chem. B* **2003**, *107* (17), 4024–4033.
(30) Virgili, J. M.; Nedoma, A. J.; Segalman, R. A.; Balsara, N. P. *Macromolecules* **2010**, *43* (8), 3750–3756.
(31) Tokuda, H.; Hayamizu, K.; Ishii, K.; Susan, M. A. B. H.; Watanabe, M. *J. Phys. Chem. B* **2005**, *109* (13), 6103–6110.
(32) Hanley, K. J.; Lodge, T. P.; Huang, C. I. *Macromolecules* **2000**, *33* (16), 5918–5931.
(33) Krummen, M.; Wasserscheid, P.; Gmehling, J. *J. Chem. Eng. Data* **2002**, *47* (6), 1411–1417.
(34) Fulcher, G. S. *J. Am. Ceram. Soc.* **1925**, *8* (12), 789–794.
(35) Fulcher, G. S. *J. Am. Ceram. Soc.* **1925**, *8* (6), 339–355.
(36) Tammann, G.; Hesse, W. *Z. Anorg. Allg. Chem.* **1926**, *156* (4) .
(37) Vogel, H. *Phys. Z.* **1921**, *22*, 645–646.
(38) Adam, G.; Gibbs, J. H. *J. Chem. Phys.* **1965**, *43* (1), 139–&.
(39) Ferry, J. D. *Viscoelastic Properties of Polymers*, 3rd ed.; John Wiley & Sons, Inc.: New York, 1980.
(40) Passaglia, E.; Kevorkian, H. K. *J. Appl. Phys.* **1963**, *34* (1), 90–&.
(41) Kirkpatr., S. *Rev. Mod. Phys.* **1973**, *45* (4), 574–588.
(42) Hunt, A. G.; Ewing, R. P. *Percolation Theory for Flow in Porous Media*; Lecture Notes in Physics; Springer: Berlin, 2009.
(43) Scher, H.; Zallen, R. *J. Chem. Phys.* **1970**, *53* (9), 3759–&.
(44) Morris, D. R.; Sun, X. D. *J. Appl. Polym. Sci.* **1993**, *50* (8), 1445–1452.
(45) Maki-Ontto, R.; de Moel, K.; Polushkin, E.; van Ekenstein, G. A.; ten Brinke, G.; Ikkala, O. *Adv. Mater.* **2002**, *14* (5), 357–361.
(46) Park, M. J.; Balsara, N. P. *Macromolecules* **2010**, *43* (1), 292–298.
(47) Noda, A.; Hayamizu, K.; Watanabe, M. *J. Phys. Chem. B* **2001**, *105* (20), 4603–4610.